

Photoactivation investigations with ^{115}In

A. Ljubičić and K. Pisk

"Ruder Boskovic" Institute, P.O. Box 1016, Zagreb, Yugoslavia

B. A. Logan

Department of Physics, University of Ottawa, Ottawa, Ontario, Canada

(Received 20 June 1980)

A ^{60}Co source has been used to study the photoactivation of the 336 keV ($T_{1/2} \sim 4.3$ h) isomeric level of ^{115}In . In contrast to earlier investigations, we have considered the possibility of nonresonant processes and have developed a technique which allows us to distinguish between activation via the resonance fluorescence of the 1078 keV ^{115}In level, and by nonresonant processes involving the 1172 and 1332 keV ^{60}Co photons. We have found that nonresonant processes are the dominant modes of activation. Although various possible mechanisms for the nonresonant excitation have been considered, none seem sufficiently strong to explain our results.

$$\left[\text{RADIOACTIVITY } ^{115}\text{In; studied photoactivation with } ^{60}\text{Co, measured } \Gamma_0 \text{ for } \right. \\ \left. 1078 \text{ keV, investigated excitation mechanism.} \right]$$

I. INTRODUCTION

The photoactivation of isomeric levels has been studied extensively.¹⁻¹⁰ The activation usually involves strong (~ 1000 Ci) γ -ray sources or the intense bremsstrahlung emitted by accelerated electron beams. In previous investigations a mechanism has been assumed in which resonant energy photons in the low energy tail associated with intense γ -ray sources, or in the continuum of the bremsstrahlung, excited higher energy levels via resonance fluorescence, and that these subsequently decayed to the isomeric level.

We have investigated the photoactivation of the 336 keV isomeric level ($T_{1/2} \sim 4.3$ h) of ^{115}In ; the level structure and the γ -ray branching scheme¹¹ of ^{115}In are given in Fig. 1. Previous studies of the photoactivation of the ^{115}In isomeric level have assumed that either the 1078 keV or the 1464 keV levels of ^{115}In were excited via resonance fluorescence, the isomeric level being populated when they decayed. Other excited levels of ^{115}In are either too narrow to be strongly excited in resonance fluorescence, or their decays do not populate the isomeric level.

We have studied the photoactivation of the ^{115}In isomeric level, using a 680 Ci ^{60}Co source, and have developed a technique to measure the probability of the isomeric level being excited in nonresonant processes as well as via the resonance fluorescence of the 1078 keV level. The possibility of nonresonant excitation does not seem to have been considered in other photoactivation investigations.

II. POSSIBLE EXCITATION MECHANISMS

A. Excitation via resonance fluorescence

The absorption cross section for an isolated level in a stationary nucleus is¹²

$$\sigma_{\text{abs}}(E) = \frac{\pi g \lambda^2 \Gamma_0 \Gamma}{2[(E - E_R)^2 + \Gamma^2/4]}, \quad (1)$$

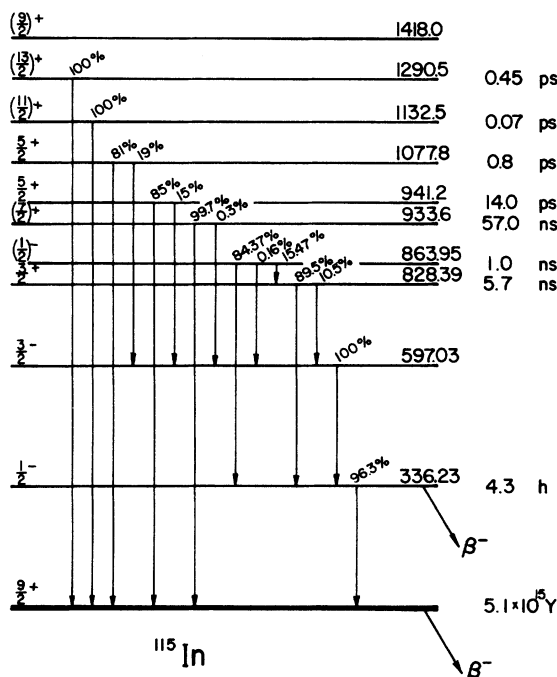


FIG. 1. The level structure and γ -ray branching scheme of ^{115}In .

where $\lambda = \hbar c/E$, E is the γ -ray energy, and $\hbar c = 1.973 \times 10^{-11}$ MeV cm. The statistical weight factor $g = (2I + 1)/(2I_0 + 1)$ and contains the total angular momenta I of the excited level and I_0 the ground state value. Γ_0 is the ground state transition width and Γ is the total width of the level.

For a continuous photon distribution the relevant quantity is

$$\int_{-\infty}^{+\infty} \sigma_{\text{abs}}(E) dE,$$

and, when Doppler broadening effects are allowed for, this reduces to $\pi^2 g \lambda^2 \Gamma_0$; this is independent of the details of the Doppler broadening. If the flux of resonant energy photons is $\phi_R(E_R)$ photons per unit area, energy, and time, the probability of exciting the level in a nucleus per unit time is

$$\pi^2 g \lambda^2 \Gamma_0 \phi_R(E_R). \quad (2)$$

For a partial width for decay to the isomeric level Γ_{iso} the probability per nucleus of exciting the isomeric level per unit time is

$$\pi^2 g \lambda^2 \Gamma_0 \phi_R(E_R) (\Gamma_{\text{iso}}/\Gamma). \quad (3)$$

For ^{115}In considerations of Γ_0 values and $\Gamma_{\text{iso}}/\Gamma$ ratios show that the 1078 keV level is the dominant intermediate level in populating the isomeric level via resonance fluorescence.

B. Excitation via nonresonant processes

If ϕ_{NR} is the number of nonresonant photons per unit area and time and $\sigma_{\text{NR}}(E_i)$ represents the cross section for nonresonant excitation of a level with an energy E_i , higher than the energy of the isomeric level, the probability of exciting the isomeric level per unit time is $\phi_{\text{NR}} \sigma_{\text{NR}}^T$. In our case ϕ_{NR} is dominated by the flux of 1172 and 1332 keV photons and has been taken as the sum of the fluxes associated with these γ rays; σ_{NR}^T represents the total cross section for exciting the isomeric level by nonresonant processes and is given by

$$\sigma_{\text{NR}}^T = \left[\sigma_{\text{NR}}(E_{\text{iso}}) + \sum \sigma_{\text{NR}}(E_i) \frac{\Gamma_{\text{iso}}(i)}{\Gamma} \right]. \quad (4)$$

III. THE TECHNIQUE FOR DISTINGUISHING BETWEEN RESONANT AND NONRESONANT PROCESSES

We have considered the possibilities of the isomeric level being excited after resonance fluorescence of the 1078 keV level or by nonresonant processes. In principle, data are available for the Γ , Γ_0 , and Γ_{iso} values and a knowledge of $\phi_R(1078)$ and ϕ_{NR} would allow the nonresonant contributions to be determined. In practice, values available for Γ and Γ_0 show wide variations and it is difficult to determine $\phi_R(1078)$. We have used

a technique which has allowed Γ_0 and σ_{NR}^T to be measured simultaneously.

Our technique involves using lead pieces interposed between the source and the indium sample during the photoactivation exposures. The Compton scattering and absorption inside the lead distorts the photon spectrum and changes the relative values of $\phi_R(1078)$ and ϕ_{NR} . The relative number of 1078 keV photons increases with lead thickness. This is illustrated in Fig. 2, which shows the variation in the fraction of photons in a 50 keV energy slice centered at 1078 keV, as compared to the number of full energy photons, as a function of lead thickness. In the photoactivation exposures the relative number of resonant excitations increases as the thickness of lead increases and by using several different thickness it is possible to distinguish between the resonant and nonresonant contributions. The data shown in Fig. 2 were obtained using a 10 μCi ^{60}Co source and by observing the different response of Ge(Li) detector as the lead pieces were interposed.

The photon flux is also distorted by absorption and scattering in the indium foil and in the plexiglass used to support the system during photoactivation. The former was investigated by measuring the change in the response of the Ge(Li) detector when the indium foil was placed between the 10 μCi ^{60}Co source and the detector. The contribution from the plexiglass was estimated to be $< 10\%$ of the indium foil's effect in producing extra photons in the 1078 keV energy region. Although the lead pieces were the dominant contribution in distorting the photon spectrum the effects of the indium and the plexiglass were allowed for.

The ^{60}Co source used in the photoactivation exposures had a strength of (680 ± 70) Ci. It occupied a volume of about 1 cm^3 and was surrounded

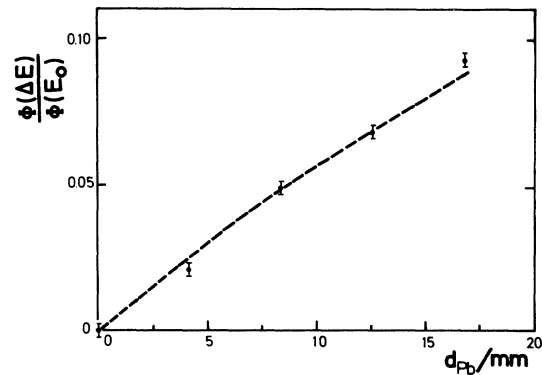


FIG. 2. The variation in the fraction of photons in a 50 keV energy slice centered at 1078 keV, as compared to the number of 1332 keV photons, as a function of lead thickness. The broken line represents the calculated value.

by substantial shielding material. The photon beam emerging from a 28 cm long collimator was expected to have an appreciable low energy tail. This was not measured directly but a parameter k , which represented the fraction of photons with less than the full energy that emerged from the source, was a variable in a χ^2 comparison between the experimental photoactivation data and the theoretical predictions. Data from the manufacturers of the source¹³ indicated that k was in the range $0.1 \leq k \leq 0.2$, but k was allowed to vary from 0–0.5 in the χ^2 analysis.

IV. PHOTOACTIVATION MEASUREMENTS

The indium sample was placed 30 cm from the source and five exposures were made: one with no lead between the source and the indium, and four with lead thickness ranging from 0.42–1.68 cm. The indium foil was 0.4 cm thick and had a diameter of 2.54 cm. The irradiation time t_{irr} was usually about 17 h.

For a lead piece with a thickness d the activity induced is $N\lambda(d, t_{irr})$ and is given by

$$N\lambda(d, t_{irr}) = N_A (1 - e^{-\lambda t_{irr}}) \times \left[\frac{\pi^2 g \lambda^2 \Gamma_0 \Gamma_{iso}}{\Gamma} \phi_R(1078, d) + \sigma_{NR}^T \phi_{NR}(d) \right], \quad (5)$$

where N_A is the number of ^{115}In nuclei in the sample, λ is the decay constant for the isomeric level, $\phi_R(1078, d)$ represents the number of photons at the resonance energy, per unit area, energy, and time, when a lead piece with thickness d is used, and $\phi_{NR}(d)$ is the number of full energy photons per unit area and time when a thickness d of lead is used.

The induced photoactivities were counted for collection times t_{coll} in a shielded 17 cm³ Ge(Li) detector; t_{coll} was ~8.3 h. There was a time delay Δt between the end of the irradiation and the start of the counting period. The number of disintegrations during t_{coll} is given by $N_R(d, t_{coll})$

$$N_R(d, t_{coll}) = \frac{N_A}{\lambda} e^{-\lambda \Delta t} (1 - e^{-\lambda t_{irr}}) (1 - e^{-\lambda t_{coll}}) \times \left[\frac{\pi^2 g \lambda^2 \Gamma_0 \Gamma_{iso}}{\Gamma} \phi_R(1078, d) + \sigma_{NR}^T \phi_{NR}(d) \right]. \quad (6)$$

The number of γ rays detected in the Ge(Li) detector in $N_\gamma(d, t_{coll})$ and is given by

$$N_\gamma(d, t_{coll}) = N_R(d, t_{coll}) \frac{\epsilon}{(1 + \alpha)} \frac{X_{gs}}{(X_{gs} + \beta^-)}. \quad (7)$$

α is the total internal conversion coefficient for the 336 keV level and was estimated¹¹ to have a

value of 1.137. The factor $X_{gs}/(X_{gs} + \beta^-) = 0.963$ and allows for the 3.7% β^- decay of the isomeric level to ^{115}Sn . ϵ is the efficiency of the Ge(Li) detector for 336 keV photons; this was measured using standard sources, the effects of the indium foil thickness and area being taken into consideration.

The data for $\phi_R(1078, d)$ and $\phi_{NR}(d)$ were based on the supplementary measurements made with the 10 μCi ^{60}Co source, only k remaining as an experimentally undetermined parameter. The value of Γ_{iso}/Γ for the 1078 keV level was taken as 0.19.¹⁴

V. χ^2 ANALYSIS

We can represent

$$\left[\pi^2 g \lambda^2 \frac{\Gamma_0 \Gamma_{iso}}{\Gamma} \phi_R(1078, d) + \sigma_{NR}^T \phi_{NR}(d) \right]$$

by $P(d)$. The χ^2 analysis compared the experimental values $P_E(d)$ with the theoretical values $P_T(d)$ for five values of d . The parameters k , Γ_0 , and σ_{NR}^T were varied to minimize

$$\chi^2 = \sum_{i=1}^5 \left[\frac{P_T(d_i) - P_E(d_i)}{\Delta P_E(d_i)} \right]^2. \quad (8)$$

$\Delta P_E(d_i)$ is the uncertainty in $P_E(d_i)$ and is dominated by uncertainties in $N_\gamma(d, t_{coll})$. χ^2 was relatively insensitive to the value of k , and a value of $k = 0.16$ was obtained, in good agreement with the source specifications. For k values between zero and 0.3, the best values of σ_{NR}^T vary by only $\pm 5\%$ from the value obtained at $k = 0.16$. For fixed k , χ^2 was sensitive to the value of σ_{NR}^T , as can be seen from Fig. 3. The sensitivity of the procedure is illustrated in Fig. 4.

VI. RESULTS AND COMPARISONS WITH PREVIOUS WORK

The values derived for Γ_0 and σ_{NR}^T are 1.43×10^{-4} eV and 3.8×10^{-31} cm², respectively, after the

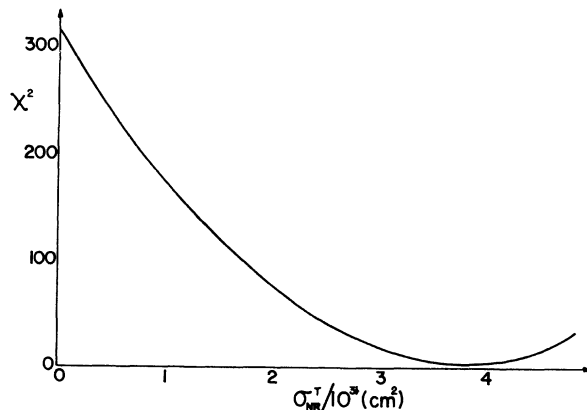


FIG. 3. The variation of the χ^2 value with the total cross section for nonresonant contributions.

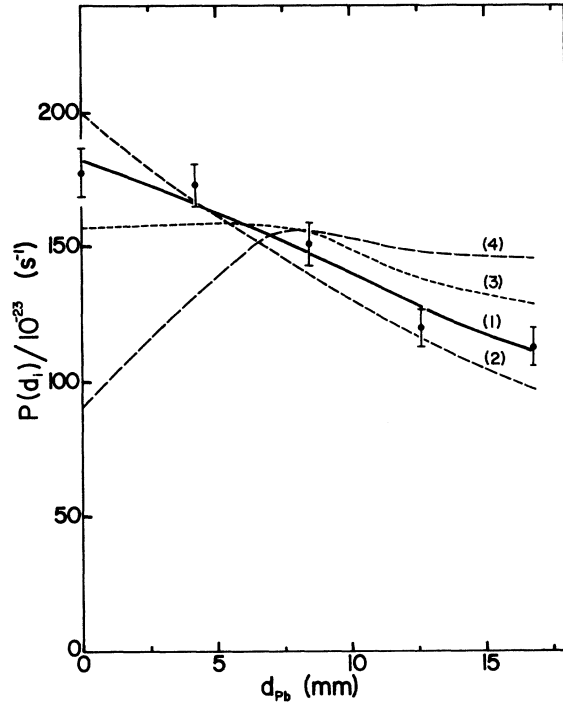


FIG. 4. A comparison of the experimental and calculated values of $P(d_i)$ as a function of d_i , the lead thickness. The lines for the calculated values are hand drawn through five calculated values. The values obtained for χ^2 , σ_{NR}^T , and Γ_0 for the various lines are (1) $\chi^2=2.95$, $\sigma_{\text{NR}}^T=3.8 \times 10^{-31} \text{ cm}^2$, $\Gamma_0=1.43 \times 10^{-4} \text{ eV}$; (2) $\chi^2=15.4$, $\sigma_{\text{NR}}^T=4.4 \times 10^{-31} \text{ cm}^2$, $\Gamma_0=0.70 \times 10^{-4} \text{ eV}$; (3) $\chi^2=22.3$, $\sigma_{\text{NR}}^T=2.9 \times 10^{-31} \text{ cm}^2$, $\Gamma_0=2.28 \times 10^{-4} \text{ eV}$; and (4) $\chi^2=178.8$, $\sigma_{\text{NR}}^T=1.0 \times 10^{-31} \text{ cm}^2$, $\Gamma_0=3.80 \times 10^{-4} \text{ eV}$. The k value was 0.16 in each case.

best χ^2 value of 2.95 was obtained. Statistical errors are 5% and, when other uncertainties are considered, the values are expected to be accurate within 12%.

Values of Γ_0 obtained in other investigations are given in Table I. The Coulomb excitation values¹⁴⁻¹⁷ assume the transition is $E2$, which is generally accepted. These values tend to be less than the values derived from experiments using continuous photon distributions.

Our results indicate that, when no lead is inserted between the ^{60}Co source and the indium sample, only 10% of the excitations of the isomeric level proceed via resonance fluorescence of the 1078 keV level. This rises to 45% when 1.68 cm of lead are inserted. This suggests that in many experimental investigations involving continuous photon distributions unconsidered nonresonant contributions could have been important and could result in an overestimate of Γ_0 .

The width of the 1078 keV level and its coupling to the isomeric level, along with theoretical con-

TABLE I. Γ_0 values for the 1078 keV level.

| Reference | Experimental technique ^a | Γ_0 (eV) |
|-----------|-------------------------------------|----------------------------------|
| 4 | Photoactivation | $(5.7 \pm 1.0) \times 10^{-4}$ |
| 6 | Photoactivation | $(2.0 \pm 0.7) \times 10^{-4}$ |
| 7 | Photoactivation | $(2.8 \pm 1.0) \times 10^{-4}$ |
| 8 | Photoactivation | $(7.4 \pm 4.7) \times 10^{-4}$ |
| 10 | Photoactivation | $(4.7 \pm 1.3) \times 10^{-4}$ |
| 14 | Coulomb excitation | $(4.3 \pm 0.4) \times 10^{-4}$ |
| 15 | Coulomb excitation | $(1.5 \pm 0.5) \times 10^{-4}$ |
| 16 | Coulomb excitation | $(1.9 \pm 0.4) \times 10^{-4}$ |
| 17 | Coulomb excitation | $(2.6 \pm 0.3) \times 10^{-4}$ |
| 18 | Resonance fluorescence | $(6.0 \pm 1.4) \times 10^{-4}$ |
| This work | | $(1.43 \pm 0.17) \times 10^{-4}$ |

^aThe Γ_0 values for the photoactivation measurements have been derived from the integrated cross section values assuming $\Gamma_{\text{iso}}/\Gamma=0.19$.

siderations outlined in the theory section, suggest that the 1078 keV level may be a dominant intermediate state in the nonresonant process. If this is so the cross section for nonresonant excitation of the 1078 keV level would be $2.0 \times 10^{-30} \text{ cm}^2$.

VII. THEORETICAL CONSIDERATIONS

Our results show that nonresonant processes are important in the excitation of the isomeric level and we have considered some possible mechanisms for nonresonant excitations. The three processes we have considered are (a) resonant absorption at energies very far from the resonant energy; (b) a possible inelastic photoelectric effect in which photoelectrons excite nuclear levels; and (c) inelastic nuclear Raman scattering. The details are outlined below.

A. Resonant adsorption

The cross section for this depends on the Γ_0 value and when the decay scheme of ^{115}In is considered only the 941 and 1078 keV $\frac{5}{2}^+$ levels could excite the isomeric level. If we use Eq. (1) the cross sections for fluorescing these levels with 1172 and 1332 keV photons are $< 1.6 \times 10^{-38} \text{ cm}^2$ in all cases; details are given in Table II. In practice, Doppler broadening spreads out the absorption cross section in the region near the resonance energy but this gives an even stronger falloff at energies far from the resonance. While we may question the accuracy of Eq. (1) at energies very

TABLE II. Calculated values for exciting the 941 and 1078 keV levels in ^{115}In for various excitation mechanisms.

| Incident photon energy (keV) | ^{115}In state (keV) | Nuclear resonance fluorescence | Cross sections for the various processes (cm^2) | | |
|------------------------------------|----------------------------------|-----------------------------------|--|------------------------------|--|
| | | | Inelastic photoelectric effect | Dynamic collective effect | Raman scattering via 1464 keV level |
| 1172 | 941 | 9.2×10^{-42} | 5.3×10^{-37} | 6.7×10^{-35} | |
| 1172 | 1078 | 1.6×10^{-38} | 4.9×10^{-37} | 1.2×10^{-36} | 4.6×10^{-40} |
| 1332 | 941 | 2.7×10^{-42} | 5.3×10^{-36} | 3.8×10^{-35} | |
| 1332 | 1078 | 1.8×10^{-39} | 5.4×10^{-36} | 6.8×10^{-36} | 3.9×10^{-38} |

far from resonance it seems reasonable to conclude that resonant absorption cross sections are many orders of magnitude below the experimental results.

B. Inelastic photoelectric effect

The inelastic photoelectric effect we have considered is a third order electromagnetic process which involves the interaction between a photon, a bound atomic electron, and the nucleus. The relevant Feynman diagram is shown in Fig. 5. The nuclear excitation is due to the interaction between the ground state nucleus and the ejected orbital electron after photoabsorption.

Details of the calculations will be presented elsewhere. Contributions from K -shell electrons are expected to dominate and our calculations are limited to these. Our calculations neglect the effect of the static Coulomb field of the nucleus on the intermediate and final electron states and only zero momentum contributions of the initial K -shell electrons are included. The cross sections are proportional to Γ_0 , as in the case of Coulomb excitation, and we have calculated the cross sections for excitation of the 941 and 1078 keV levels for this process; the results are given in Table II. The values are several orders of magnitude below our experimental results.

C. Nuclear Raman scattering

Nuclear Raman scattering is a second order process in the electromagnetic interaction of the

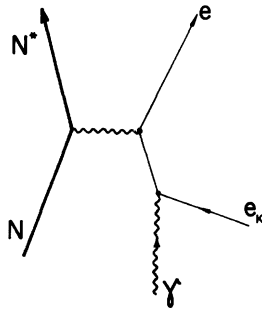


FIG. 5. The Feynman diagram for the inelastic photoelectric effect.

nucleus. The description of the dynamics of this process involves second order perturbation theory and in principle all possible nuclear intermediate states should be considered. At higher photon energies it has been established that the intermediate state is the giant dipole resonance (GDR).

Various models are available for cross section calculations. ^{115}In is a vibrational nucleus and the most appropriate model is the dynamic collective model (DCM). The scattering cross section for dipole scattering by unoriented nuclei is given by^{19, 20}

$$\frac{d\sigma_{\text{DCM}}}{d\Omega} = \frac{1}{2I_0 + 1} \frac{E'}{E} \sum_{j=0}^2 g_j |P_j|^2. \quad (9)$$

In this expression, E' is the energy of the scattered photon. The functions g_j represent the kinematic properties of the scattering process, where j is the angular momentum transfer to the nucleus; the g 's are

$$\begin{aligned} g_0 &= \frac{1}{6} (1 + \cos^2\theta), \\ g_1 &= \frac{1}{4} (2 + \sin^2\theta), \\ g_2 &= \frac{1}{12} (13 + \cos^2\theta). \end{aligned} \quad (10)$$

P_j represents the nuclear dipole polarizabilities,

$$\begin{aligned} P_j &= (-)^j \cdot I_0 \cdot I_f \cdot E E' \sum_n \left\{ \begin{matrix} 1 & j \\ I_0 & I_f & I_n \end{matrix} \right\} \langle I_f | |D| | I_n \rangle \langle I_n | |D| | I_0 \rangle \\ &\quad \times \left[\frac{1}{E_n + E' + \frac{1}{2} i \Gamma_n} + \frac{(-)^j}{E_n - E - \frac{1}{2} i \Gamma_n} \right] \\ &\quad - \delta_{j0} \delta_{if} \delta_{EE'} 3(2I_0 + 1) \frac{Z^2 e^2}{A M c^2}, \end{aligned} \quad (11)$$

where I_n , E_n , and Γ_n represent the spins, energies, and widths of the intermediate states. The reduced matrix elements of the dipole operator D are defined within the collective model.

Although the existing equations involving the GDR can be used at low energies it is not clear as to how meaningful this is at energies as low as 1 MeV. Even though we realize this is of doubtful validity we have made calculations assuming a GDR intermediate state. We have assumed that any direct coupling between the single-particle

isomeric level state and the GDR is negligible and have calculated the cross sections for populating the 941 and 1078 keV levels. The data given by Arenhövel and Maison²¹ for inelastic photon scattering by ^{115}In has been used to extract GDR parameters and reduced dipole matrix elements. Although this extraction was made visually the procedure should be sufficient to determine if our results can be described in terms of the dynamic collective model. The calculated cross sections are given in Table II.

Hayward²² has also made an estimate of the cross section. The coherent elastic scattering cross section has a real and imaginary part, and while the imaginary part is negligible below the particle emission threshold, the real part combines with the Thomson amplitude to produce the total amplitude. If the giant resonance is represented as a single Lorentz line, then the real part of the forward scattering amplitude is

$$\frac{\Gamma\sigma_0}{4\pi\hbar c} \frac{E^2(E_r^2 - E^2)}{[(E_r^2 - E^2)^2 + \Gamma^2 E^2]}.$$

Using the parameters of Berman and Fultz,²³ $\Gamma = 5.24 \text{ MeV}$, $\sigma_0 = 266 \text{ mb}$, and $E_r = 15.63$; at 1332 keV this amplitude is $\sim 4 \times 10^{-17} \text{ cm}$.

An inspection of the elastic and inelastic photon scattering cross sections for vibrational nuclei^{21,24} reveals that the inelastic scattering cross section is about one-fourth the elastic scattering cross section. The forward inelastic scattering amplitude would then be half the value for elastic scattering and would be $\sim 2 \times 10^{-17} \text{ cm}$. The forward inelastic cross section would be $\sim 4 \times 10^{-34} \text{ cm}^2/\text{sr}$ and the total inelastic cross section would be $\sim 5 \times 10^{-33} \text{ cm}^2$. This estimate is still too small to be consistent with our experimental result.

It is also possible to disregard the GDR picture and consider isolated low energy intermediate states. In this case the dipole operator is connected with the measured transition rates between the intermediate states and the levels being considered. States which involve dipole-dipole absorption are of interest and we have made a calculation assuming the 1464 keV $\frac{1}{2}^+$ level as an intermediate state. This level has a measured transition probability to the 1078 keV level; the

calculated values for the two photon energies are given in Table II.

VIII. CONCLUSIONS

We have developed a technique to distinguish between resonant and nonresonant contributions in the photoactivation of isomeric levels. It has been established that the photoactivation of the 336 keV isomeric level of ^{115}In involves a dominant contribution from nonresonant processes. Earlier investigations have not considered the possibility of nonresonant contributions, and values of Γ_0 derived from them may be suspect.

Although we have considered possible processes for nonresonant excitation of ^{115}In levels, all of our theoretical predictions are several orders of magnitude below our experimental result. In the case of the dynamic collective model it is difficult to have much confidence at energies as low as 1 MeV; more detailed calculations would be of some interest. The inelastic photoelectric effect is an interesting physical phenomenon but the cross section is too low to explain our results.

If, as seems possible, the 1078 keV level is dominantly involved in the nonresonant processes, this creates difficulties in the conventional description of some resonance fluorescence measurements made with continuous energy photon sources. In some experimental arrangements corrections would have to be made to allow for nonresonant contributions and Γ_0 values which have been derived may be incorrect.

It is of interest to investigate other isomeric levels in different nuclei in order to find if nonresonant contributions are always important in photoactivation investigations. Further experiments are now in progress to resolve this question.

ACKNOWLEDGMENTS

The irradiations were carried out using a ^{60}Co facility at the National Research Council in Ottawa; Dr. W. H. Henry is thanked for his advice and assistance concerning these irradiations. One of us (B.A.L.) would like to thank the Natural Sciences and Engineering Research Council of Canada for financial support.

¹B. Pontecorvo and A. Lazard, *C. R. Acad. Sci.* **208**, 99 (1939).

²G. B. Collins, B. Waldman, E. M. Stubblefield, and M. Goldhaber, *Phys. Rev.* **55**, 507 (1939).

³G. Harbottle, *Nucleonics* **12**, 64 (1954).

⁴K. Yoshihara, *Isot. Radiat. Technol.* **3**, 472 (1960).

⁵A. Veres, I. Pavlicsek, M. Csuros, and L. Lakosi, *Acta Phys. Acad. Sc. Hung.* **34**, 97 (1973).

⁶B. T. Chertok and E. C. Booth, *Nucl. Phys.* **66**, 230 (1965).

⁷E. C. Booth and J. Brownson, *Nucl. Phys.* **A98**, 529 (1967).

- ⁸M. Boivin, Y. Cauchois, and Y. Heno, Nucl. Phys. A137, 520 (1969).
⁹M. Boivin, Y. Cauchois, and Y. Heno, Nucl. Phys. A176, 626 (1971).
¹⁰Y. Watanabe and T. Mukoyama, Bull. Inst. Chem. Res. Kyoto Univ. 57, 72 (1979).
¹¹S. Raman and H. J. Kim, Nucl. Data Sheets 16, 195 (1975).
¹²F. Metzger, Prog. Nucl. Phys. 7, 54 (1959).
¹³W. H. Henry (private communication).
¹⁴F. S. Dietrich, B. Herskind, R. A. Naumann, and R. G. Stokstad, Nucl. Phys. A155, 209(1970).
¹⁵D. G. Alkhazov, K. I. Erokhina, and I. Kh. Lemberg, Izv. Akad. Nauk SSSR, Ser. Fiz. 28, 1667 (1964).
¹⁶J. McDonald, D. Porter, and D. T. Stewart, Nucl. Phys. A104, 177 (1967).
¹⁷E. M. Bernstein, G. G. Seaman, and J. M. Palms, Nucl. Phys. A141, 67 (1970).
¹⁸W. J. Alston III, Phys. Rev. 188, 1837 (1969).
¹⁹E. G. Fuller and E. Hayward, Nucl. Phys. 30, 613 (1962).
²⁰U. Fano, NBS Technical Report No. 83 (1960).
²¹H. Arenhövel and J. M. Maison, Nucl. Phys. A147, 305 (1970).
²²E. Hayward (private communication).
²³B. L. Berman and S. C. Fultz, Rev. Mod. Phys. 47, 713 (1975).
²⁴H. Arenhövel and H. J. Weber, Nucl. Phys. A91, 145 (1967).